Pergamon

PII: S0042-6989(96)00094-6

Vision Res., Vol. 36, No. 22, pp. 3629–3639, 1996

Printed in Great Britain
0042-6989/96 $15.00 + 0.00

Assimilation-type and Contrast-type Bias of Motion Induced by the Surround in a Random-dot Display: Evidence for Center–Surround Antagonism

IKUYA MURAKAMI,*‡ SHINSUKE SHIMOJO†

Received 7 August 1995; in revised form 22 February 1996

As a mechanism to detect differential motion, we have proposed a model of "a motion contrast detector" that has a center–surround antagonistic receptive field with respect to the direction of motion. Supporting evidence has been obtained in the studies of induced motion, motion capture, and motion aftereffect. In order to obtain further evidence in a more strictly controlled situation, we examined the perceptual bias of motion in a center stimulus induced by another, surrounding motion. By using a stochastic random-dot display configured in a center–surround concentric fashion, we measured the % signal in the center stimulus that made the stimulus perceptually stationary in the presence of a moving surround. Measurements were done for various stimulus sizes and eccentricities. The amount of bias changed as a function of stimulus size and eccentricity. At several eccentricities, smaller stimulus sizes tended to yield assimilation-type biases, whereas larger sizes tended to yield contrast-type biases. However, a spatial scaling procedure revealed that the amount of bias was a simpler function of "scaled" stimulus size that was obtained by dividing the physical size by a scaling factor at each eccentricity. In the scaled profile, assimilation-type bias changed to contrast-type bias with increasing size, reached the peak of contrast-type bias at a certain size, and decreased slightly with further increasing size. Furthermore, a model of a difference of Gaussians, DOG, function well approximated the behavior of the profile. From these results, we concluded that the process specific to perceiving relative motion is mediated by a motion contrast detector, which is possibly located in area MT. Copyright © 1996 Elsevier Science Ltd.

Motion perception Contrast and assimilation Scaling factor Center–surround antagonism Area MT

INTRODUCTION

Motion in the retinal image is used for various visual functions (Nakayama, 1985). These include segregating moving objects from their background, extracting the contour of objects, and recovering depth and three-dimensional structure. Evidently, the information processing involved in achieving these functions requires mechanisms sensitive to the relative motion between adjacent points in the image. In the present study, we aim to show human psychophysical evidence for the existence of a local mechanism that detects motion which is opposite in direction to that of its surround.

A psychophysically feasible way to explore the possibility that such a mechanism exists is to examine whether motion perception within one region in the image is influenced by the motion surrounding that region. Induced motion (sometimes referred to as perceptual "contrast" in motion), the illusory motion of a stationary stimulus in the direction opposite to its moving surround, has been studied extensively in this context by a number of researchers [see Reinhardt-Rutland (1988) for review]. Some of them have proposed, as its underlying mechanism, a directionally antagonistic unit that is inhibited by moving stimuli in the surround (Anstis & Reinhardt-Rutland, 1976; Loomis & Nakayama, 1973; Nakayama & Tyler, 1978; Nawrot & Sekuler, 1990; Reinhardt-Rutland, 1981, 1983; Strelow & Day, 1975; Tynan & Sekuler, 1975; Walker & Powell, 1974). We will tentatively call such a motion processing unit "a

*Department of Psychology, Division of Humanities, University of Tokyo, Tokyo, Japan.

†Department of Psychology, College of Arts and Sciences, University of Tokyo, Tokyo, Japan.

‡To whom all correspondence should be addressed at: Laboratory of Neural Control, National Institute for Physiological Sciences, Myodaiji, Okazaki, Aichi 444, Japan [*Fax* +81 564 55 7865; *Email* ikuya@nips.ac.jp].

motion contrast detector". We use the term "motion contrast" for the difference in physical velocities between adjacent regions in the visual field [as originally defined by Regan & Beverley (1984)].

Ramachandran (1987) reported a phenomenon called motion capture (sometimes referred to as perceptual "assimilation" in motion), the illusory motion of a stationary equiluminant stimulus in the same direction as its moving surround. Murakami and Shimojo (1993b) have recently found that when the overall size of the stimulus was decreased, induced motion could change to motion capture, even if the stationary stimulus was not equiluminant. Furthermore, the critical size at which induced motion changes to motion capture differed across eccentricities. To interpret these results, Murakami and Shimojo (1993b) suggested that a population of the detectors is distributed around a certain stimulus size at each eccentricity—a stimulus of the optimal size results in a percept due to relative motion processing (induced motion). A smaller stimulus, where both the inducer and the induced stimulus are within the center field, results in another percept due to nonselective pooling of motion information below the resolution limit (motion capture).

Since induced motion has often been *explained* by such a hypothetical mechanism having center–surround antagonism, the next step is to *test* the hypothesis that such a mechanism exists in the human visual system. For this purpose, an adaptation paradigm would be promising. After prolonged exposure to an adapting stimulus moving in one direction, a stationary stimulus appears to move in the direction opposite to that of the adapting stimulus (Wohlgemuth, 1911). This effect, called motion aftereffect, has been taken as strong evidence for a mechanism specialized for motion processing (Blakemore & Campbell, 1969). Murakami and Shimojo (1995) examined how an inducing stimulus in a surround modulates the motion aftereffect in a central stimulus. There were two adapting gratings in a center-surround configuration. The direction of the surround grating was either the same as or opposite to the direction of the center. They found a "surround modulation" of the motion aftereffect, i.e. the adaptation to two opposite motions in the center and surround elicited a larger motion aftereffect in the center than did the adaptation to the same unidirectional motion in the two fields. The results could not be interpreted in terms of unidirectional motion detectors. Instead, they strongly suggested the existence of processing units sensitive to relative motion.

So far, evidence supporting the motion contrast detector has been reported using suprathreshold illusions: induced motion; motion capture; and motion aftereffect. Although these are useful psychophysical tools which have been used to investigate the units in the motion processing system, one should be cautious in extrapolating illusion-based results to more strict situations such as the motion detection threshold. In the present study, we attempted to "replicate" the experiment on the stimulus size- and eccentricity-dependences of induced motion/motion capture (Murakami & Shimojo, 1993b). While the original study qualitatively determined how *strongly* these illusions were perceived, here we quantitatively determined and measured the bias (a shift of the psychometric function) on the motion perception of the center stimulus in the presence of a moving surround. (If the psychometric function is biased in the direction in which the center more readily appears to move together with the surround, it is a perithreshold counterpart of motion capture. If the bias is opposite, it is a perithreshold counterpart of induced motion.) The bias turned out to vary with both size and eccentricity. We also examined whether the apparent dependence on eccentricity could reflect a simpler effect relating to cortical size when the data were rescaled using a linear scaling factor. A successful spatial scaling would make it likely that local mechanisms are embedded in some stages where retinotopy is preserved, and that they are different across various eccentricities only in scale. This hypothetical structure would also be consistent with our previous studies (Murakami & Shimojo, 1993b, 1995), where the data obtained for various stimulus sizes and various eccentricities seemed to obey a simpler function of scaled stimulus size. The results of the present study were then compared with previous psychophysical studies on the spatial interaction between biasing and biased stripes (Chang & Julesz, 1984; Nawrot & Sekuler, 1990).

METHODS

Subjects

One of the authors and one naive subject participated. Both had normal or corrected-to-normal vision.

Equipment

The experiment was done in a dark room. The stimulus was presented on a CRT monitor (Apple 13" CRT; 640×480 pixels; vertical scanning frequency 66.7 Hz, noninterlaced) controlled by a personal computer (Apple Macintosh Quadra 840AV). The subject used only his right eye with a natural pupil, with the left eye occluded by an eye-patch. The subject's head was stabilized with a chin rest.

Stimulus

We attempted to obtain a psychometric curve as a function of some magnitude of motion signal in the stimulus. We adopted a sparse random-dot pattern in which a certain percentage of dots ("signal dots") moved coherently in one direction while others ("noise dots") moved in random directions and with random speeds (Newsome & Paré, 1988)*. The display was an apparent

*The size of each dot was small and the density of dots was rather high when compared to those used in previous studies that used similar stimuli in the recording of the macaque MT neurons (Britten *et al.*, 1993; Newsome & Paré, 1988; Salzman *et al.*, 1992). We chose this density because it would permit many dots to be within the receptive field of a single unit in the macaque V1, and directional judgment could be mediated by processing levels lower than MT.

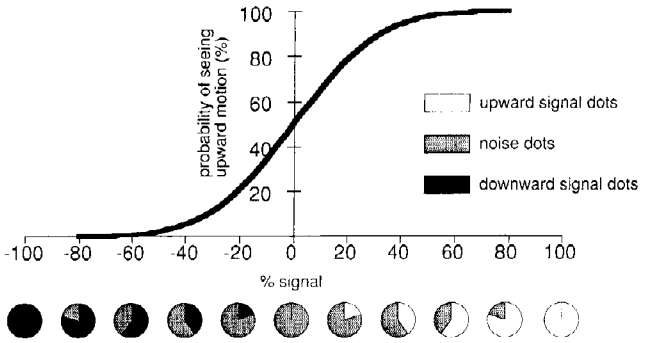

FIGURE 1. A schematic view of a psychometric function. Assume that the nominal signal direction of the display is upward and that the observer judges the direction (upward or downward) in which the display appears to move. All dots are noise at 0% signal. The number of upward signal dots increases as % signal moves from 0 to 100. The number of downward signal dots increases as % signal dots decreases from 0 to −100. The ordinate of the psychometric function indicates the probability of seeing upward motion. The psychometric curve is expected to be a sigmoid function of this signed % signal. The pie charts below the abscissa illustrate the percentage of component dots in the display at each level of % signal. When there is no moving surround, it is expected that the psychometric function will pass through the 50% probability at 0% signal. When there is a biasing surround, it is expected that the function will be shifted laterally and consequently, the % signal that yields 50% probability will depart from 0%.

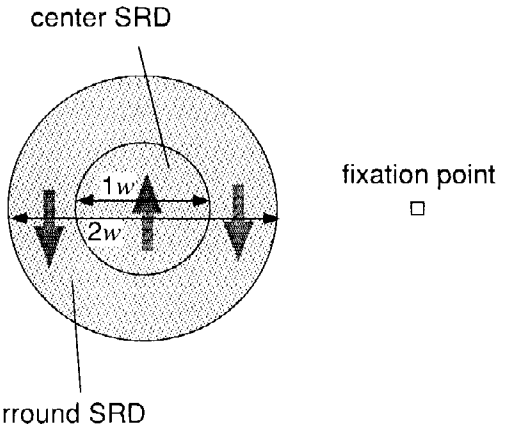

FIGURE 2. A schematic view of stimulus configuration. Two SRDs were organized concentrically. The center SRD (comprising white dots) was confined to the region of the inner disk. The surround (comprising red dots) was confined to the region of the outer annulus. In this annular window, 50% of the dots in the surround SRD moved coherently in the upward direction in half the trials, and moved coherently in the downward direction in the other half. The other 50% of the dots were noise dots. The % signal of the center SRD was "positive" if the signal dots moved in the same direction as the signal in the surround, and was "negative" if they moved in the opposite direction to those in the surround. The eccentricity was varied by changing the location of the fixation point. The parameter for stimulus size, w, was varied by changing the viewing distance.

motion stimulus, i.e. it comprised many static monitor frames refreshed successively. In a frame, f, a certain percentage ("% signal") of dots were assigned to be signal dots, whereas other dots were assigned to be noise dots. In the next frame, $f+1$, the signal dots shifted in a certain direction ("signal direction") by a certain distance, whereas the noise dots jumped to a new position chosen randomly. When % signal = 100, a global motion was perceived in the display in the direction of the signal dots. When % signal = 0, the display was perceived as dynamic noise, although there were many local motion components in random directions and at random speeds. When % signal was between $0 \sim 100\%$, the probability of seeing global motion in the signal direction increased monotonically with increasing % signal. A concept of *negative* % signal was also introduced in order to denote the percentage of signal dots moving in the opposite direction to the original. For instance, let the upward direction be chosen as the nominal signal direction. Decreasing the % signal from 100% to 0% would decrease the proportion of upward-moving signal dots to randomly moving noise dots. Further decreasing the % signal from 0% to −100% would increase the proportion of downward-moving signal dots (opposite direction to the nominal signal) to randomly moving noise dots. Such notation was useful in plotting a psychometric curve of directional judgment as a function of one-dimensional scale (Fig. 1). A psychometric curve would range from no upward response at a very low (negative) % signal, to perfect upward response at a very high (positive) % signal. This random-dot display, with a signal range of $-100 \sim 100\%$, will hereafter be called "stochastic random-dot display (SRD)".

Two SRDs were located concentrically on a dark background in the nasal visual field (Fig. 2). Their sizes were controlled by one parameter, w. One SRD was confined to a disk-shaped static window whose diameter was $1w$ and was called "center SRD". The other was confined to an annulus-shaped static window surrounding the center SRD and was called "surround SRD". The diameters of the inner and outer circles of the annulus were $1w$ and $2w$, respectively. This size relationship was chosen on the basis of the data in our pilot studies, though larger outer diameters were just as good. The surround SRD comprised red (18.8 cd/m^2) dots; 50% of all the dots were signal dots and the others were noise dots; the signal direction was upward in some trials and downward in other trials. The center SRD comprised white (101 cd/m^2) dots; its nominal signal direction was the same as that of the surround SRD. Recall the % signal concept we introduced previously. If we let the signal direction of the surround SRD be upward, positive % signals in the center SRD would correspond to the situations in which some dots move upward and others move randomly. Negative % signals would correspond to the situations in which some dots move downward and others move randomly.

The color difference was introduced merely to help the perceptual segregation between the center and surround. (If the only difference was in % signal, the subject would have had difficulty in determining the border between them, especially if they had similar values of % signal.) Other than the color and the % signal, all of the other

parameters were identical for both SRDs.* The luminance of the background was about 0.01 cd/m^2, the density was $50/w^2$ dots/deg^2, the nominal diameter of each dot was $1w$ min (1 pixel served as one dot), and the velocity of signal dots was $4w$ min/frame, where w was a parameter for the stimulus size.† The duration of one frame was 30 msec, the inter-frame interval was 0 msec, the number of frames was 15, and the total exposure time was 450 msec. New SRDs were generated for each trial.

The parameter for the stimulus size, w, was varied in eight steps (0.5, 0.75, 1, 1.5, 2, 3, 4, 5, 8) by varying the viewing distance from 15.8 to 252.3 cm. The eccentricity was defined as the distance from the fixation point (a white square generated graphically) to the center of the stimulus and was varied in six steps (0, 2, 3, 4.5, 6, 9) by varying the location of the fixation point.

Procedure

The size and the eccentricity were constant during each experimental session. The signal direction of the surround SRD (upward/downward) was chosen randomly from trial to trial. The % signal of the center SRD was also chosen randomly, from five levels of % signal which differed by steps of 20% (e.g. –30, –10, 10, 30, and 50). These had been chosen in advance and roughly determined the dynamic range of a psychometric function according to the results of our preliminary experiments.

The subject was required to keep foveating the fixation point on the dark background. The concentric SRDs were presented at the left of the fixation point. The subject's task was to judge the perceived direction of the center SRD in a two-alternative forced-choice task (upward/downward). The subject's response triggered the inter-trial interval (450 ± 225 msec).

The % signal which yielded equal probabilities for upward motion perception and downward motion perception, hereafter referred to as the "PSE" (point of subjective equality to the stationary state), was determined for each stimulus size and eccentricity. The probability of seeing the same direction as the surround was calculated on the basis of 32 repeated trials and was plotted against % signal. The curve was fitted to the logistic function

$$y = \frac{1}{1 + \exp[-\beta_0(x - \beta_1)]} \qquad (1)$$

to obtain a sigmoid curve, where y denotes probability and x denotes % signal. The regression coefficient β_0 corresponds to the steepness of the curve and β_1 corresponds to the % signal which yields the probability of 50%. The coefficients were obtained separately for the case of upward surround and for the case of downward surround. Because no systematic difference was found between the two values of β_1 obtained in these two cases, they were averaged and their mean was taken as a final estimate of PSE.

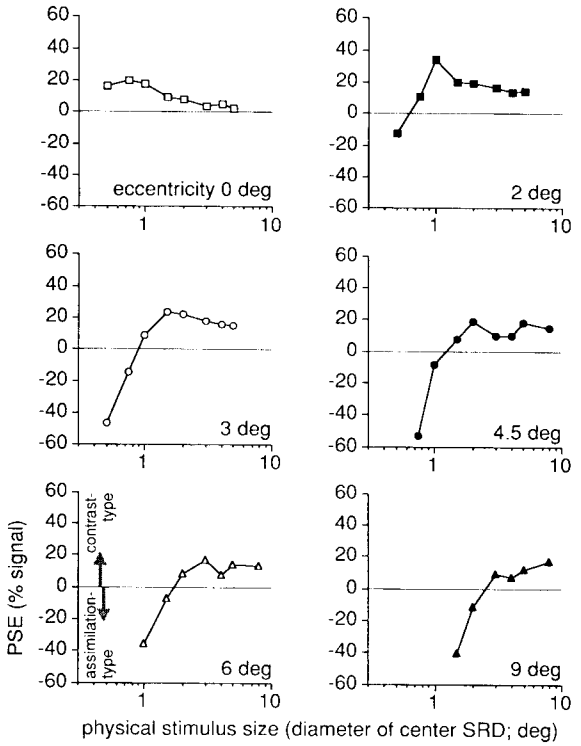

FIGURE 3. The PSE (% signal that yielded a 50% probability of seeing upward motion) obtained for various stimulus sizes and eccentricities. The data are for subject IM. The PSE is plotted against w on a logarithmic scale. Each panel corresponds to each eccentricity tested. Positive PSEs indicate contrast-type bias and negative PSEs indicate assimilation-type bias.

RESULTS

The PSEs determined for various stimulus sizes at various eccentricities are shown in Fig. 3 (for subject IM) and in Fig. 4 (for subject SM). The data for each eccentricity are plotted in separate panels. The PSE is plotted against the parameter for stimulus size, w (= the diameter of the center SRD), using a logarithmic scale. Negative PSEs indicate that the subject more readily observed the center moving in the same direction as the surround. Therefore, they will be referred to as assimilation-type biases. Positive PSEs indicate the opposite and will be referred to as contrast-type biases.

The data shown in Figs 3 and 4 clearly indicate that the stimulus size affected the PSE differently at different eccentricities. At 0 deg eccentricity, the PSE was positive (contrast-type bias) for all stimulus sizes and showed a flat or slightly declining curve. At other eccentricities, the polarity of the PSE changed from negative to positive

*Their motion detection thresholds were not identical, but very similar. For example, subject IM's motion detection threshold (75% correct in a two-alternative forced-choice task) under typical conditions (a circular field with 3 deg diameter at 4.5 deg eccentricity) was about 9% coherence for white, and about 11% for red. The 50% coherence case yielded almost perfect detectability even for red dot fields. Similar results were obtained at other sizes and eccentricities.

†In a pilot experiment, results that were quantitatively similar to the main results were obtained for subject IM when the dot density and the dot velocity were 0.25 and 2 times as large, respectively, as in the main experiment.

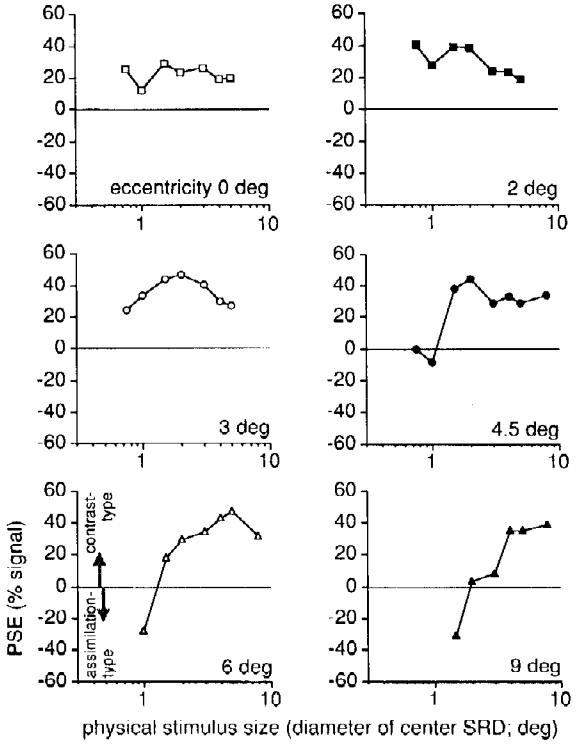

FIGURE 4. The data for subject SM. Formats are identical to Fig. 3.

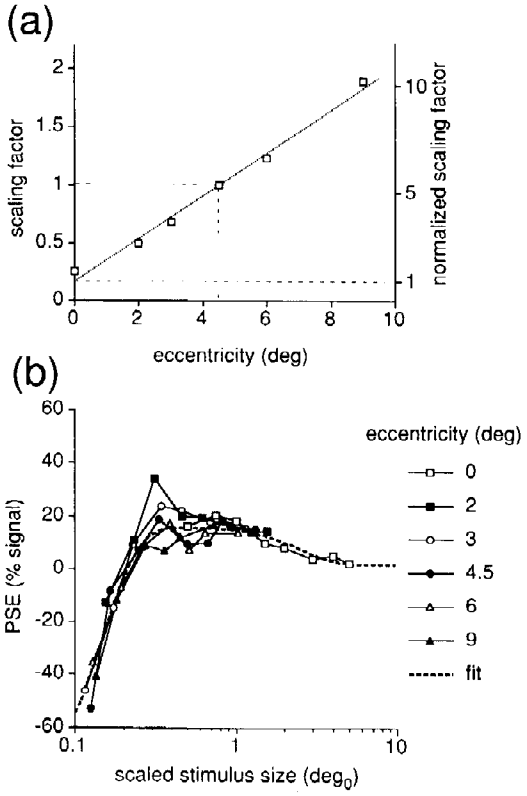

FIGURE 5. The spatial scaling analysis for subject IM. (a) The scaling factor estimated for each eccentricity. The factor is 1 for 4.5 deg eccentricity by definition, and therefore the linear regression line is constrained to pass through (4.5, 1). The right-hand ordinate indicates the scaling factor normalized such that the line passes through (0, 1). (b) The PSE data replotted as a function of scaled stimulus size. The stimulus size at each eccentricity is divided by the normalized scaling factor as shown in (a). The data for various eccentricities are overlaid. The broken line indicates the fitted curve [Eq. (2)].

with increasing stimulus size. At 3 deg eccentricity, the PSE seemed to lie on an inverted-U curve. At 9 deg eccentricity, the curve became less steep with increasing size. The data for other eccentricities seemed to have intermediate effects along with some fluctuations. To summarize, the PSE changed as a function of stimulus size and eccentricity and there seemed to be a complex interaction between these two factors.

A careful observation of the data suggests that the shapes of the profiles show relatively systematic changes with increasing eccentricity. For example, the curve at 9 deg eccentricity appears to be the result of a lateral shift of the 6 deg curve. Also, the 2 deg curve and the 6 deg curve partially overlap the right half and left half, respectively, of the 3 deg curve, after they have been laterally shifted by an appropriate amount. If the psychophysical function of stimulus size at a given eccentricity can be considered to be a lateral shift of another psychophysical function at another eccentricity along the log axis of stimulus size, it can be said that the functions are spatially scalable (Watson, 1987). A successful spatial scaling in turn suggests that the underlying mechanisms at different eccentricities are qualitatively identical but different only in scale. We examined whether the apparent dependence on eccentricity reflected a simpler effect of scaled stimulus size when the data were scaled using a linear scaling factor.

Since we did not know what kind of fitting function or physiological knowledge is appropriate, we chose to apply a knowledge-free procedure introduced by Whitaker *et al.* (1992). Using the least squares method iteratively, this procedure calculates the scaling factor such that the profiles for different eccentricities best agree with each other [see Appendix A; see also Murakami & Shimojo (1995)]. Assuming that the scaling factor should be a linear function of eccentricity [see Drasdo (1991)], the factors that were estimated for individual eccentricities were fitted to a linear regression line.

The above analysis resulted in a normalized scaling factor $F = 1 + 1.116E$ for subject IM [Fig. 5(a)] and $F = 1 + 0.989E$ for subject SM [Fig. 6(a)], where F denotes the scaling factor and E denotes the eccentricity (deg). Dividing the physical size by this estimated scaling factor [right-hand ordinates in Figs 5(a) and 6(a)] at each eccentricity, we obtain the scaled size (deg_0), where the unit deg_0 denotes 1 deg at the fovea. When the data are plotted using these scaled values, a remarkable (though imperfect) agreement across eccentricities is obvious [Figs 5(b) and 6(b)]. The residual disagreement can be interpreted as a noise, since no systematic deviation exists. Also, the degree of agreement can be described objectively in terms of the determination coefficient (R^2) in the following fitting procedure.

The scaled data seemed to be on a single inverted-U-shaped function: the PSE was negative for small sizes,

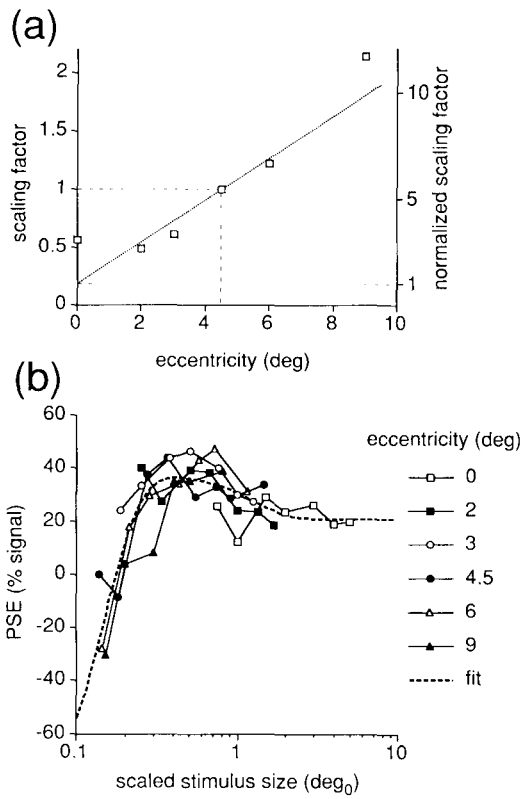

FIGURE 6. The spatial scaling analysis for subject SM. The format is identical to that in Fig. 5.

met the zero-crossing at about 0.2 deg_0, reached the peak at about 0.4 deg_0, and slightly decreased with further increasing size. In an attempt to determine the peak of this function, these data were fitted to the function

$$y = f(w) = a + b\left[4\int_0^{w/2} \mathrm{DOG}(t)\mathrm{d}t - 2\int_0^{w} \mathrm{DOG}(t)\mathrm{d}t\right], \quad (2)$$

where DOG(x) is a difference of two Gaussians

$$\mathrm{DOG}(x) = \mathrm{N}\left(\frac{x}{\sigma_c}\right) - k\mathrm{N}\left(\frac{x}{\sigma_s}\right), \quad (3)$$

N(x) is a standard Gaussian function, y denotes PSE, and w denotes the stimulus size. For further details of the theoretical implication of the above equation, see Appendix B, but it should be mentioned here that the estimated σ_c and σ_s are indices of the spatial extents of center and surround subregions of the motion contrast detector model. The results of this fitting procedure were (a, b, k, σ_c, σ_s) = (–82.1, 98.0, 0.143, 0.0604, 1.000) for subject IM (R^2 = 0.91) and (a, b, k, σ_c, σ_s) = (–89.6, 127.2, 0.129, 0.0606, 0.500) for subject SM (R^2 = 0.71). The fitted curves are superimposed on Figs 5(b) and 6(b) (dotted lines). Their peaks are at 0.373 deg_0 for IM and 0.352 deg_0 for SM. If one assumes that the peak of the inverted-U function approximates the situation in which contrast-type bias occurred maximally irrespective of eccentricity, the parameter for the stimulus size w that yields the maximum contrast-type bias is $w = 0.373(1 + 1.116E)$ for IM and $w = 0.352(1 + 0.989E)$ for SM, where E denotes eccentricity. Since these estimated coefficients are not too different between subjects, they are averaged and result in

$$w = 0.363(1 + 1.05E). \quad (4)$$

These results suggest that the cortical mechanisms underlying the present experimental task are identical across eccentricities except for the preferred stimulus size. Since the scaled bias × size function seems to show band-pass characteristics [see Figs 5(b) and 6(b)], it suggests that the underlying mechanism is a band-pass filter in the motion domain, such as center–surround antagonism with respect to preferred direction.

DISCUSSION

In the present study, perithreshold psychophysical performance was examined and the results support an idea suggested by previous experiments using suprathreshold illusions such as induced motion, motion capture, and motion aftereffect (Murakami & Shimojo, 1993b, 1995). The idea is that the difference in motion signals between adjacent visual fields is detected by motion contrast detectors whose receptive field profiles have center–surround antagonism in the motion domain. The results are also consistent with the notion that these hypothetical detectors are distributed across eccentricities, whose preferred stimulus size increases with increasing eccentricity. If we assume that the stimulus size that yields the maximum contrast-type bias is the same size of the center subregion of the receptive field, Eq. (4) gives the estimate of the spatial extent of the center subregion. Also, the data suggest that the spatial extent of the surround subregion is much larger than the center, since σ_s was 8 ~ 16 times as large as σ_c in the fitted DOG function.

In the following discussion, we will compare the present finding with previous studies. The effect of stimulus size on a stripe version of motion capture was studied by Chang and Julesz (1984). They examined the perceived direction of a test random-dot pattern, whose direction was physically ambiguous. When random dots in flanking stripes moved unambiguously, the perceived direction of the test pattern was biased towards the same direction as these inducing stripes. This assimilation-type bias was limited to a certain distance: the maximally effective stripe width was about 0.25 deg at the fovea. Our data are consistent with their estimation at least qualitatively, in that assimilation-type bias occurs in a limited range in space. Their estimation and our data would be also similar in a quantitative sense, if the diameter of our center SRD is equivalent to their stripe width. The curves shown in Figs 5(b) and 6(b) indicate that when the diameter of the center SRD exceeded 0.21 deg_0 for subject IM [Fig. 5(b)] and 0.17 deg_0 for SM [Fig. 6(b)], assimilation-type bias disappeared (although we did not obtain actual data for the size of about 0.2 deg

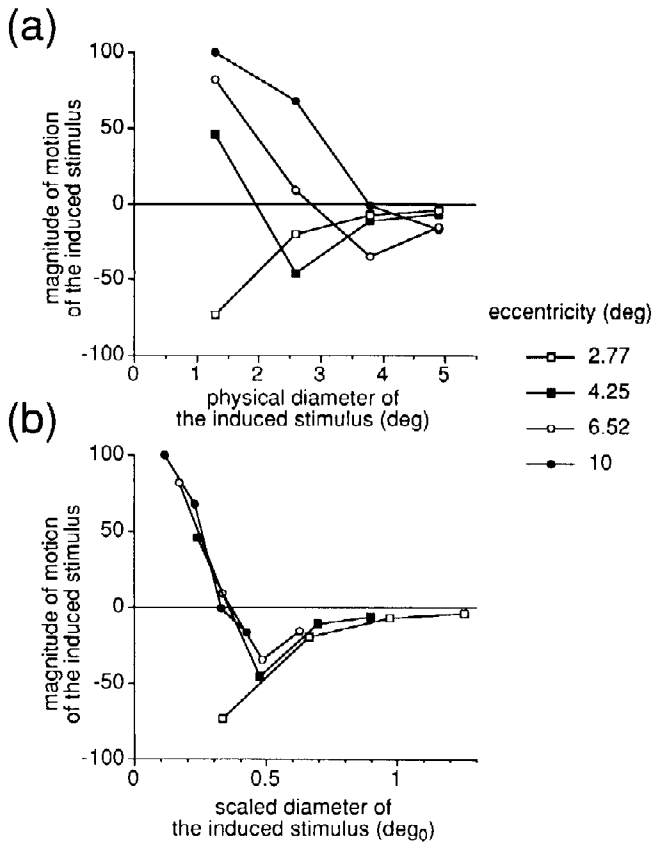

FIGURE 7. The original data of Murakami and Shimojo (1993b) and the replotted chart using the scaling factor estimated in the present study. (a) The estimated magnitude of the perceived motion of the induced stimulus is plotted as a function of the stimulus size. A positive magnitude indicates that the induced stimulus appears to move in the same direction as the inducer (i.e. motion capture), whereas a negative magnitude indicates that the induced stimulus appears to move in the direction opposite to the inducer (i.e. induced motion). (b) The abscissa is changed to the scaled stimulus size according to the estimated scaling factor $F = 1 + 1.05E$.

at 0 deg eccentricity). These values resemble the estimation by Chang and Julesz (1984).

Two previous studies have shown that assimilation-type bias changed to contrast-type bias when the stimulus size was increased (Murakami & Shimojo, 1993b; Nawrot & Sekuler, 1990). Murakami and Shimojo (1993b) used a central stationary disk as an induced stimulus and a moving random-dot pattern as an inducer, and found that at about $4 \sim 6.5$ deg eccentricity, motion capture (assimilation) changed to induced motion (contrast) when the overall stimulus size was increased. They also scaled their data for $2.77 \sim 10$ deg eccentricities by dividing the stimulus size by the receptive field size of MT neurons (Albright & Desimone, 1987), since this cortical area seemed to be the most likely candidate for the neural implementation of motion contrast detectors, as we will discuss later. Their scaling method was reasonably successful [Fig. 7(b) in their article], but we will attempt to scale their data by using the scaling factor estimated in the present study ($F = 1 + 1.05E$), in order to see the applicability of our current estimate to the previous study. Their original data are shown in Fig. 7(a), and the scaled version is plotted in Fig. 7(b), where the abscissa is the diameter of the induced stimulus in terms of deg_0. The ordinates indicate magnitude estimates of the perceived motion of the induced stimulus; the positive values correspond to the magnitude of motion capture and the negative values correspond to the magnitude of induced motion. The scaling procedure yields a good agreement across eccentricities except for just one point. The zero-crossing is located at about 0.3 deg_0, which is more or less consistent with the present study and also with the study by Chang and Julesz (1984). The negative peak is located at about 0.5 deg_0, which is a bit greater than the estimated peak of 0.363 deg_0 in the present study.

Nawrot and Sekuler (1990) examined spatial interaction between biasing stripes and ambiguous stripes in foveal vision. Their stimulus configuration was similar to that used in the study by Chang and Julesz (1984). Their main finding was qualitatively in accordance with the present study, in that assimilation-type bias changed to contrast-type bias with increasing stimulus size (stripe width). Their estimates of the effective stripe width (where motion assimilation changed to contrast) was, however, at least three times as large as Chang and Julesz's (1984) estimate, and was also not consistent with ours. The reason for this quantitative discrepancy is unclear, but we can speculate that the size of their display area, which subtended 2.5×4.8 deg, might have allowed the maximum eccentricity of 2.4 deg to contribute to the performance. In our present study, according to Eq. (4), the scaling factor at 2.4 deg eccentricity is 3.52 times larger than the foveal one. Thus, the effective size of the spatial interaction found in the present study is consistent with the size estimated by Nawrot and Sekuler (1990), if one assumes that they actually measured the size of spatial interaction at 2.4 deg eccentricity. This might account for the apparently longer spatial interaction in their report.

Various scaling factors have been reported to explain apparent differences in motion perception at different eccentricities. For comparison, they are plotted in a single chart, Fig. 8, in normalized forms [see Eq. (6) in Appendix A], i.e. they pass through (0, 1) such that the factor is unity at the fovea. These scaling factors include the ones found in the study by Levi *et al.* (1984) who measured the detection thresholds for absolute motion [Fig. 8(i)] and for relative motion [Fig. 8(d)] in separate experiments, the study by McKee and Nakayama (1984) who measured the detection threshold for relative motion [Fig. 8(e)], the study by Wright and Johnston (1985) who measured the magnitude of motion aftereffect using absolute motion [Fig. 8(g)], the study by Murakami and Shimojo (1995) who measured the magnitude of motion aftereffect using relative motion [Fig. 8(c)], and the present study [Fig. 8(a and b)]. At a first glance, these scaling factors appear diverse, although more careful observation leads to the impression that psychophysical performances related to absolute motion tend to have

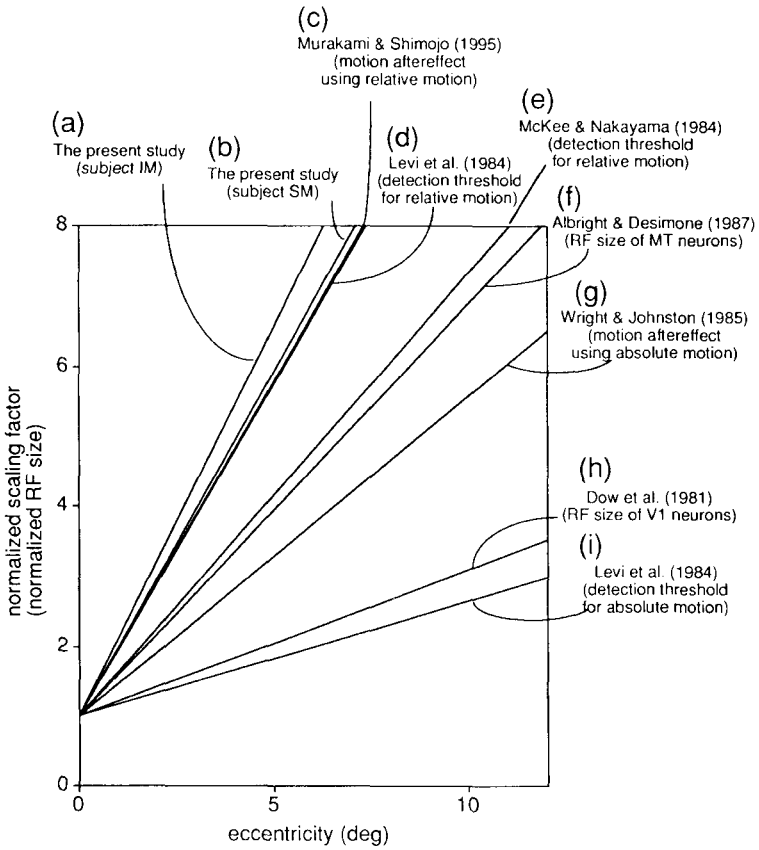

FIGURE 8. The scaling factor estimated in the present study and its relationship to previous studies. All scaling factors and receptive field sizes are normalized to pass through (0, 1) just for comparison. (a) The present study, for subject IM. (b) The present study, for subject SM. (c) The scaling factor estimated by Murakami and Shimojo (1995) in the study of modulation of motion aftereffect by surrounding motion: $F = 0.148 + 0.142E$. (d) The scaling factor estimated by Levi *et al.* (1984) in the study of detection threshold for relative motion: $F = 1 + 1.05^{-1}E$. (e) The scaling factor estimated by McKee and Nakayama (1984) in the study of detection threshold for relative motion: $F \approx 1 + 0.63E$. (f) The receptive field size of MT neurons of the macaque measured by Albright and Desimone (1987), on which the spatial scaling of the original study by Murakami and Shimojo (1993b) was based. (g) The scaling factor used in the study by Wright and Johnston (1985): $F = 1 + 0.42E + 0.00012E^3$, approximated as a linear function ($F = 0.953 + 0.434E$) in this range for the sake of comparison. (h) The receptive field size (RF) of V1 neurons of the macaque measured by Dow *et al.* (1981): $\log_{10}(RF \times 60) = 1.1438 + 0.1920x + 0.0712x^2 + 0.0619x^3$, where $x = \log_{10}(E \times 60) - 1.5$, approximated as a linear function $RF = 0.232 + 0.0488E$ in this range for the sake of comparison. (i) The scaling factor estimated by Levi *et al.* (1984) in the study of detection threshold for absolute motion: $F = 1 + 5.99^{-1}E$.

shallow slopes whereas performances related to relative motion tend to have steeper slopes. Since the idea of the scaling factor is based on physiological knowledge about the eccentricity-dependence of cortical magnification and receptive field sizes, such differences in slope suggest that absolute motion and relative motion are processed in distinct cortical areas, though further investigation must be done.

A great number of physiological studies in the monkey have revealed that many neurons in V1 are directionally selective, i.e. they prefer a certain direction of motion presented in their receptive fields [e.g. Hubel & Wiesel (1968)]. Most of the neurons in MT are directionally selective too, but some of them have more properties than just directional selectivity. Their responses to their preferred motion are suppressed when motion in the same direction is presented in the surround of their classical receptive fields [e.g. Tanaka *et al.* (1986)]. As these physiological characteristics are very similar to the expected behavior of the hypothetical motion contrast detector, it is natural to consider this subtype of MT neuron as the most likely candidate for the neural correlate of the motion contrast detector. Also, the present model of the motion contrast detector matches another property of MT neurons. The fitted DOG function indicates that the surround subregion of the detector is much larger than the center subregion. In the study of MT neurons of the owl monkey, Allman *et al.* (1985a) reported that the area of the suppressive surround was 50 ~ 100 times the area of the classical receptive field. A similar finding was reported in the study of the macaque's MT neurons as well (Tanaka *et al.*, 1986).

On the other hand, we should not neglect the fact that there are some quantitative disagreements between the physiological data and our psychophysical estimates.

First, the scaling factor estimated in the present study and the receptive field size of MT neurons do not match perfectly. In Fig. 8, the eccentricity-dependence of the receptive field sizes in the macaque's V1 (Dow *et al.*, 1981) and MT (Albright & Desimone, 1987) neurons are normalized and plotted together for comparison [Fig. 8 (f and h)]. The receptive field size of MT neurons show a steeper slope compared to those of V1 neurons, and our slopes are even steeper. Second, the spatial extent of the center subregion (0.363 deg in our estimation) is quite small compared to the classical receptive fields of MT neurons, though it is consistent with previous psychophysical studies (Chang & Julesz, 1984; Murakami & Shimojo, 1993b). Such a small receptive field size is not compatible with any physiological data for MT currently available (Albright & Desimone, 1987; Desimone & Ungerleider, 1986; Gattass & Gross, 1981; Komatsu & Wurtz, 1988; Maunsell & Van Essen, 1987; Tanaka *et al.*, 1986, 1993). For example, the eccentricity-dependence of receptive field sizes in the study by Albright and Desimone (1987) gives a diameter of 1.04 deg at the fovea. One possible explanation for these discrepancies is an interspecies difference in receptive field sizes between the human and monkeys. Another possibility is that it is not adequate for the present study to use the receptive field size reported previously; their data were based on area MT as a whole, while there has been a report that the neurons having center–surround antagonism are clustered in distinct columns (Born & Tootell, 1992). Also, it should be noted that the receptive field size is highly dependent on how receptive fields are mapped, hence the inconsistency in absolute size between physiology and psychophysics should not reject the significance of the present study. At the same time, however, one should be careful to note that, although the antagonism-like directionality has been studied most extensively in MT (Allman *et al.*, 1985a; Born & Tootell, 1992; Lagae *et al.*, 1989; Tanaka *et al.*, 1986), similar response characteristics have been found in other cortical areas besides MT, such as V1 and V2 of the monkey (Allman *et al.*, 1985b; Jones *et al.*, 1995). Another important caution is that direct comparison between neural activity in MT and animal behavior has yet to be investigated more in this context (Born *et al.*, 1995). Thus, the model of MT neurons which we have proposed in the present study is only hypothetical and is currently being researched.

In conclusion, the present study revealed psychophysical evidence for motion contrast detectors in a strictly controlled situation. Their characteristics are consistent with previous models which explain induced motion and motion capture (Murakami & Shimojo, 1993b), and motion aftereffect (Murakami & Shimojo, 1995). This model is also in accordance with previous psychophysical studies on motion segmentation (Chang & Julesz, 1984; Murakami & Shimojo, 1993b; Nawrot & Sekuler, 1990), and is biologically plausible as well [e.g. Allman *et al.* (1985a); Tanaka *et al.* (1986)].

REFERENCES

Abramowitz, M. & Stegun, I. A. (1965). *Handbook of mathematical functions*. New York: Dover Publications.

Albright, T. D. & Desimone, R. (1987). Local precision of visuotopic organization in the middle temporal area (MT) of the macaque. *Experimental Brain Research, 65*, 582–592.

Allman, J., Miezin, F. & McGuinness, E. (1985a). Direction- and velocity-specific responses from beyond the classical receptive field in the middle temporal visual area (MT). *Perception, 14*, 105–126.

Allman, J., Miezin, F. & McGuinness, E. (1985b). Stimulus specific responses from beyond the classical receptive field: Neurophysiological mechanisms for local–global comparisons in visual neurons. *Annual Review of Neuroscience, 8*, 407–430.

Anstis, S. M. & Reinhardt-Rutland, A. H. (1976). Interactions between motion aftereffects and induced movement. *Vision Research, 16*, 1391–1394.

Blakemore, C. B. & Campbell, F. W. (1969). On the existence of neurones in the human visual system selectively sensitive to the orientation and size of retinal images. *Journal of Physiology, 203*, 237–260.

Born, R. T., Groh, J. M. & Newsome, W. T. (1995). Functional architecture of primate area MT probed with microstimulation: Effects on eye movements. *Society for Neuroscience Abstracts, 21*, 281.

Born, R. T. & Tootell, R. B. H. (1992). Segregation of global and local motion processing in primate middle temporal visual area. *Nature, 357*, 497–499.

Britten, K. H., Shadlen, M. N., Newsome, W. T. & Movshon, J. A. (1993). Responses of neurons in macaque MT to stochastic motion signals. *Visual Neuroscience, 10*, 1157–1169.

Chang, J. J. & Julesz, B. (1984). Cooperative phenomena in apparent movement perception of random-dot cinematograms. *Vision Research, 24*, 1781–1788.

Desimone, R. & Ungerleider, L. G. (1986). Multiple visual areas in the caudal superior temporal sulcus of the macaque. *Journal of Comparative Neurology, 248*, 164–189.

Dow, B. M., Snyder, A. Z., Vautin, R. G. & Bauer, R. (1981). Magnification factor and receptive field size in foveal striate cortex of the monkey. *Experimental Brain Research, 44*, 213–228.

Drasdo, N. (1991). Neural substrates and threshold gradients of peripheral vision. In Kulikowski, J. J., Walsh, V. & Murray, I. J. (Eds), *Limits of vision* (pp. 251–265). Hampshire: Macmillan Press.

Gattass, R. & Gross, C. G. (1981). Visual topography of striate projection zone (MT) in posterior superior temporal sulcus of the macaque. *Journal of Neurophysiology, 46*, 621–638.

Hubel, D. H. & Wiesel, T. N. (1968). Receptive fields and functional architecture of monkey striate cortex. *Journal of Physiology, 195*, 215–243.

Jones, H. E., Grieve, K. L. & Sillito, A. M. (1995). Spatial organisation and selectivity of the interacting components underlying responses of cells highlighting discontinuity or intersections in the visual world. *Society for Neuroscience Abstracts, 21*, 1653.

Komatsu, H. & Wurtz, R. H. (1988). Relation of cortical areas MT and MST to pursuit eye movements. I. Localization and visual properties of neurons. *Journal of Neurophysiology, 60*, 580–603.

Lagae, L., Gulyás, B., Raiguel, S. & Orban, G. A. (1989). Laminar analysis of motion information processing in macaque V5. *Brain Research, 496*, 361–367.

Levi, D. M., Klein, S. A. & Aitsebaomo, P. (1984). Detection and discrimination of the direction of motion in central and peripheral vision of normal and amblyopic observers. *Vision Research, 24*, 789–800.

Loomis, J. M. & Nakayama, K. (1973). A velocity analogue of brightness contrast. *Perception, 2*, 425–428.

Maunsell, J. H. R. & Van Essen, D. C. (1987). Topographic organization of the middle temporal visual area in the macaque monkey: Representational biases and the relationship to callosal connections and myeloarchitectonic boundaries. *Journal of Comparative Neurology, 266*, 535–555.

McKee, S. P. & Nakayama, K. (1984). The detection of motion in the peripheral visual field. *Vision Research, 24*, 25–32.

Murakami, I. & Shimojo, S. (1993a). Detection threshold for motion contrast depends on cortically-scaled stimulus size, regardless of eccentricity. *Investigative Ophthalmology and Visual Science, 34*, 1034.

Murakami, I. & Shimojo, S. (1993b). Motion capture changes to induced motion at higher luminance contrasts, smaller eccentricities, and larger inducer sizes. *Vision Research, 33*, 2091–2107.

Murakami, I. & Shimojo, S. (1995). Modulation of motion aftereffect by surround motion and its dependence on eccentricity and stimulus size. *Vision Research, 35*, 1835–1844.

Nakayama, K. (1985). Biological image motion processing: A review. *Vision Research, 25*, 625–660.

Nakayama, K. & Tyler, W. (1978). Relative motion induced between stationary lines. *Vision Research, 18*, 1663–1668.

Nawrot, M. & Sekuler, R. (1990). Assimilation and contrast in motion perception: Explorations in cooperativity. *Vision Research, 30*, 1439–1451.

Newsome, W. T. & Paré, E. B. (1988). A selective impairment of motion perception following lesions of the middle temporal visual area (MT). *Journal of Neuroscience, 8*, 2201–2211.

Ramachandran, V. S. (1987). Interaction between colour and motion in human vision. *Nature, 328*, 645–647.

Regan, D. & Beverley, K. I. (1984). Figure–ground segregation by motion contrast and by luminance contrast. *Journal of the Optical Society of America A, 1*, 433–442.

Reinhardt-Rutland, A. H. (1981). Peripheral movement, induced movement, and aftereffects from induced movement. *Perception, 10*, 173–182.

Reinhardt-Rutland, A. H. (1983). Aftereffect of induced rotation: Separation of inducing and static areas, and monocular component. *Perceptual and Motor Skills, 56*, 239–242.

Reinhardt-Rutland, A. H. (1988). Induced movement in the visual modality: An overview. *Psychological Bulletin, 103*, 57–71.

Salzman, C. D., Murasugi, C. M., Britten, K. H. & Newsome, W. T. (1992). Microstimulation in visual area MT: Effects on direction discrimination performance. *Journal of Neuroscience, 12*, 2331–2355.

Strelow, E. R. & Day, R. H. (1975). Visual movement aftereffect: Evidence for independent adaptation to moving target and stationary surround. *Vision Research, 15*, 117–121.

Tanaka, K., Hikosaka, K., Saito, H., Yukie, M., Fukada, Y. & Iwai, E. (1986). Analysis of local and wide-field movements in the superior temporal visual areas of the macaque monkey. *Journal of Neuroscience, 6*, 134–144.

Tanaka, K., Sugita, Y., Moriya, M. & Saito, H. (1993). Analysis of object motion in the ventral part of the medial superior temporal area of the macaque visual cortex. *Journal of Neurophysiology, 69*, 128–142.

Tynan, P. & Sekuler, R. (1975). Simultaneous motion contrast: Velocity, sensitivity and depth response. *Vision Research, 15*, 1231–1238.

Walker, P. & Powell, D. J. (1974). Lateral interaction between neural channels sensitive to velocity in the human visual system. *Nature, 353*, 732–733.

Watson, A. B. (1987). Estimation of local spatial scale. *Journal of the Optical Society of America A, 4*, 1579–1582.

Whitaker, D., Rovamo, J., Macveigh, D. & Mäkelä, P. (1992). Spatial scaling of vernier acuity tasks. *Vision Research, 32*, 1481–1491.

Wohlgemuth, A. (1911). On the after-effect of seen movement. *British Journal of Psychology, 1*, 1–117.

Wright, M. J. & Johnston, A. (1985). Invariant tuning of motion aftereffect. *Vision Research, 25*, 1947–1955.

Acknowledgements—The results of a pilot experiment involving this research were presented elsewhere (Murakami & Shimojo, 1993a). We thank Grace Chang for helpful assistance to improve the English. Preparation of this article was supported by the JSPS fellowship for Japanese Junior Scientists to I. Murakami and by grants from the Ministry of Education, Science and Culture (Japan) and from the Human Frontier Science Program to S. Shimojo.

APPENDIX A

Estimation of Scaling Factor

In an attempt to rescale the physical stimulus size into some "cortical" stimulus size, we apply a knowledge-free procedure introduced by Whitaker *et al.* (1992). In the analysis for the present study, the data at an intermediate eccentricity, 4.5 deg, were taken as the "master", against which the data at other eccentricities were scaled. First, the profiles for 4.5 deg and for another eccentricity, x deg, were superimposed. Second, an approximation to the scaling factor was estimated by eye, while the data at x deg were scaled and replotted using various factors. Third, a more precise estimate of the factor was determined by using polynomial regression. The 4.5 deg and x deg data were merged and fitted to a single third-order polynomial regression curve (the choice of this particular regression is not crucial) and the sum of the squares of the residuals were calculated. Then the x deg data were scaled with a slightly different factor and the same procedure was repeated to find a scaling factor that minimized the sum of the squares of the residuals. This factor was taken as the scaling factor estimated empirically at x deg eccentricity. The data at 0, 2, 3, 6, and 9 deg eccentricities underwent this procedure, whereas the master data of 4.5 deg eccentricity were scaled to themselves by a factor of 1 by definition. The scaling factors obtained at various eccentricities were then fitted to a linear regression line constrained to go through 1 at 4.5 deg eccentricity:

$$(f - 1) = s(e - 4.5), \tag{A1}$$

where f and e denote the scaling factor and eccentricity, respectively, and s is the regression coefficient.

The above analysis yielded $s = 0.185$ for subject IM ($R^2 = 0.990$) and $s = 0.181$ for subject SM ($R^2 = 0.859$). The regression was quite successful for subject IM [Fig. 5(a)]; even for subject SM [Fig. 6(a)], the R^2 value for this linear regression was quite good, though the points at eccentricities 0 and 9 deg suggested that a second-order polynomial regression would lessen the residuals. For convenience, Eq. (A1) was normalized to the form

$$F = 1 + SE, \tag{A2}$$

so that the scaling factor at the fovea was unity. This minor transformation resulted in a normalized scaling factor $F = 1 + 1.116E$ for subject IM [Fig. 5(a), right-hand ordinate] and $F = 1 + 0.989E$ for SM [Fig. 6(a), right-hand ordinate].

APPENDIX B

Fit to the Integral of DOG

In an attempt to determine the peaks of the profiles in Figs 5(b) and 6(b), the data were fitted to a nonlinear function which included the integrals of DOG functions. This procedure was based on these three major assumptions.

1. The receptive field of a motion contrast detector is double-opponent with respect to the preferred direction, such that the center subregion is excited by upward motion and inhibited by downward motion, and the surround subregion is excited by downward motion and inhibited by upward motion [Fig. B1(b and c)].
2. The total activity of one detector is expressed as a linear summation of the excitation/inhibition profiles in space. For the sake of simplicity, when the spatial summation along one dimension only is considered, the response to the stimulus shown in Fig. B1(a) is the sum of the shaded areas in Fig. B1(b and c).

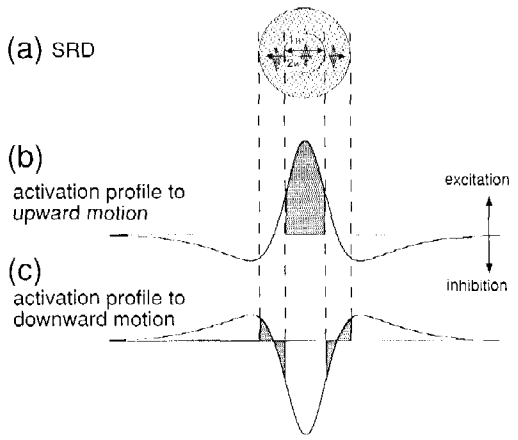

FIGURE B1. A schematic view of the relationship between the stimulus and the activation profiles of a motion contrast detector that is tuned to upward-center, downward-surround motion contrast. (a) The stimulus that is a bit smaller than the optimal one for the detector whose activation profiles are illustrated below. (b) The detector's activation profile to upward motion. The detector is excited (positive) by upward motion in the center subregion of its receptive field, and is inhibited (negative) by upward motion in the surround subregion. (c) The detector's activation profile to downward motion. The profile has the same shape but the opposite polarity compared with (b). In this model, total activation is expressed as the sum of the shaded areas (i.e. integrals of DOG functions). The detector is excited maximally by the stimulus whose center SRD matches the center subregion of the receptive field.

3. The psychophysical performance is approximated by the total response of one detector located concentrically with the stimulus. This assumption implies that the sum of the shaded areas is proportional to the data shown in Figs 5(b) and 6(b).

On the basis of these three assumptions, the shaded areas in Fig. B1, as a function of stimulus size, are chosen to be a fitting model. As a profile of center–surround antagonism, a DOG function

$$\mathrm{DOG}(x) = \mathrm{N}\left(\frac{x}{\sigma_c}\right) - k\mathrm{N}\left(\frac{x}{\sigma_s}\right) \tag{B1}$$

is chosen, where N is a standard Gaussian

$$\mathrm{N}(x) = \frac{1}{\sqrt{2\pi}}\exp\left[-\frac{x^2}{2}\right] \tag{B2}$$

and the parameters σ_c and σ_s control the spatial extents of the center and surround subregions, respectively. Also, its integral is a cumulative Gaussian (Abramowitz & Stegun, 1965)

$$\begin{aligned}\mathrm{P}(x) &= \int_{-\infty}^{x} \mathrm{N}(t)\mathrm{d}t \\ &= \frac{1}{2} + \frac{1}{\sqrt{2\pi}}\sum_n \frac{(-1)^n x^{2n+1}}{n!2^n(2n+1)}\end{aligned} \tag{B3}$$

The shaded areas in Fig. B1 are formulated as the sum of the response to the center SRD and the response to the surround SRD, and these SRDs are assumed to move in opposite directions to each other. Assuming that the sensitivities to upward motion and downward motion can be considered to have the same shapes with opposite polarities [as illustrated in Fig. B1(b and c)], the formal expression of the fitting function is

$$\begin{aligned}f(w) &= a + b\left[\int_{-w/2}^{w/2}\mathrm{DOG}(t)\mathrm{d}t - 2\int_{w/2}^{w}\mathrm{DOG}(t)\mathrm{d}t\right] \\ &= a + b\left[4\int_{0}^{w/2}\mathrm{DOG}(t)\mathrm{d}t - 2\int_{0}^{w}\mathrm{DOG}(t)\mathrm{d}t\right],\end{aligned} \tag{B4}$$

and the integrals of DOG functions in this expression can be calculated by using

$$\begin{aligned}\int_0^x \mathrm{DOG}(t)\mathrm{d}t &= \int_0^x \mathrm{N}\left(\frac{t}{\sigma_c}\right)\mathrm{d}t - k\int_0^x \mathrm{N}\left(\frac{t}{\sigma_s}\right)\mathrm{d}t \\ &= \left[\mathrm{P}\left(\frac{x}{\sigma_c}\right) - \frac{1}{2}\right] - k\left[\mathrm{P}\left(\frac{x}{\sigma_s}\right) - \frac{1}{2}\right].\end{aligned} \tag{B5}$$

For the data for each subject [Figs 5(b) and 6(b)], the vector (a, b, k, σ_c, σ_s) that minimized the sum of the squares of the residuals was determined using the method of steepest descent.